Phonon generation by current-carrying nanostructures

H. Totland
Department of Physics, University of Oslo, P. O. Box 1048 Blindern, N-0316 Oslo, Norway

Y. M. Galperin
Department of Physics, University of Oslo, P. O. Box 1048 Blindern, N-0316 Oslo, Norway
and Solid State Physics Department, A. F. Ioffe Institute, 194021 Saint Petersburg, Russia

V. L. Gurevich
Solid State Physics Department, A. F. Ioffe Institute, 194021 Saint Petersburg, Russia
(Received 7 January 1998; revised manuscript received 26 August 1998)

We calculate the rate of acoustic phonon generation by a current-carrying, ballistic quantum channel, defined in a two-dimensional electron gas by a split gate. Both uniform and nonuniform channels are considered. The generation rate of acoustic phonons of a particular frequency and direction of propagation is a steplike function of the applied bias voltage, with threshold voltages that are calculated in the paper. The emitted phonons have a characteristic angular distribution, which changes significantly at the thresholds. The voltage dependence of the generation rate is shown to be sensitive to the shape of the channel. Thus, the spectral and spatial distributions of the emitted phonons bear information both on electron-phonon coupling in the vicinity of the device and on characteristics of the electron spectrum. [S0163-1829(99)02904-5]

I. INTRODUCTION

Electronic properties of nanostructures can be effectively investigated by making use of the interaction between electrons and phonons. There has been done much experimental work on the response of nanostructures to nonequilibrium ballistic phonons and to surface acoustic waves. See for example, Refs. 1 and 2 and references therein. In this paper, however, we concentrate on the reverse effect, namely on the emission of acoustic phonons from a nanostructure carrying an electric current. The purpose of the paper is to investigate the spectral and spatial distribution of generated phonons as a function of the voltage across a one-dimensional (or quasi-one-dimensional) channel. The concrete results are obtained for the case of a channel defined in a two-dimensional electron gas (2DEG) at the interface of a semiconductor heterostructure by means of a split gate at negative potential. Phonon emission from various nanostructures has been extensively studied (see, e.g., Refs. 3 and 4 and references therein). However, we are not aware of any work on emission of acoustic phonons from a biased quantum wire.

Using the Landauer-Büttiker-Imry approach,[5] we consider a ballistic quantum channel that connects two thermal reservoirs, each being in an independent equilibrium state. As was recently shown,[6] most of the heat from a current through the channel is generated in the reservoirs.[7] Nevertheless, because of finite electron-phonon interaction inside the channel, part of the heat should be generated by the nanostructure itself via emission of phonons. In the equilibrium there is a detailed balance between the emitted and absorbed phonons. However, our situation is nonequilibrium, as the distributions of electrons penetrating into a biased quantum channel from the leads are characterized by different chemical potentials. Therefore, the phonon emission prevails over the absorption. Such phonon emission results in nothing else than the aforementioned generation of heat inside a ballistic nanostructure.

It is a complicated problem to calculate the electron-phonon coupling constant for a realistic nanostructure because of position-dependent screening (see discussion in Sec. III). We do not attempt here to solve it and assume the coupling constant to be known.

In Sec. II we consider phonons that are generated inside a long, uniform channel. The effects of smooth edges are considered in Sec. III. As a result, one can describe the phonon emission from realistic quantum channels, which usually contain a long uniform part with smoothly increasing width near the edges.

II. UNIFORM CHANNEL

In a uniform channel, the electron states can be represented as

$$\psi_{np}(\mathbf{r}) = \mathcal{L}^{-1/2}\chi_n(\mathbf{r}_\perp)\exp(ipx/\hbar),$$

where the normalization length $\mathcal{L}$ is assumed as the channel length (i.e., the distance over which the potential drops), x and $\mathbf{r}_\perp$ are the longitudinal and transverse directions respectively, p is the x component of the electron quasimomentum, and $\chi_n(\mathbf{r}_\perp)$ is the wave function of transverse quantization, the energy being

$$\epsilon_n(p) = \epsilon_n^0 + p^2/2m.$$

Here m is the electron effective mass, and $\epsilon_n^0 \equiv \epsilon_n(p=0)$ is the bottom of the nth transverse band. To be concrete, we consider a channel defined by a split-gate in a GaAs-$Al_xGa_{1-x}As$ heterostructure, and therefore, assume the system to be mechanically uniform in the direction per-

pendicular to the interface. Consequently, we consider bulk 3D acoustic phonons with the displacement $\propto \exp(i\mathbf{q}\cdot\mathbf{r})$. This assumption should be modified in the case of acoustically nonuniform quantum wires where confined modes can be present (see, e.g., Ref. 8). However, the main features of phonon generation remain similar. The matrix element for phonon-induced transitions is defined as $C_{nn'}(\mathbf{q}_\perp) = \langle \chi_{n'} | \exp(-i\mathbf{q}_\perp \mathbf{r}_\perp) | \chi_n \rangle$, where $\mathbf{q}$ is the phonon wave vector.

The number of phonons with wave vector $\mathbf{q}$, $N_\mathbf{q}(\mathbf{r},t)$, is given by the solution of the Boltzmann equation for phonons (see, e.g., Ref. 9),

$$\frac{\partial N_\mathbf{q}}{\partial t} + \mathbf{s}\nabla N_\mathbf{q} = \mathcal{R}.$$

The phonon generation is described by the collision operator $\mathcal{R} = (\partial N_\mathbf{q}/\partial t)_{\rm coll}$, which can be written as[6]

$$\mathcal{R} = \frac{2}{\mathcal{A}} \sum_{nn'} \int d\xi_p W_\mathbf{q} |C_{nn'}(\mathbf{q}_\perp)|^2 \times [f_{n,p+\hbar q_x}(1-f_{n'p})(N_\mathbf{q}+1) - f_{n'p}(1-f_{n,p+\hbar q_x})N_\mathbf{q}] \times \delta[\epsilon_n(p+\hbar q_x) - \epsilon_{n'}(p) - \hbar\omega_\mathbf{q}]. \quad (1)$$

Here $\mathbf{s} = \partial\omega_\mathbf{q}/\partial\mathbf{q}$ is the group sound velocity, $d\xi_p = dp/2\pi\hbar$, $\mathcal{A} = \mathcal{V}/\mathcal{L}$ is the cross section of the channel ($\mathcal{V}$ being its volume), while the factor 2 comes from the summation over electron spin (we assume all the transition probabilities to be spin-independent). The coupling coefficient $W_\mathbf{q}$ for the piezoelectric coupling is (cf. with Ref. 10) $W_\mathbf{q} = (\pi/\rho\omega_\mathbf{q})[e\beta_{q,lq}\nu_l(\mathbf{q},a)/\epsilon_{qq}\epsilon_0]^2$. Here e is the electron charge, $\beta_{i,ln}$ is the tensor of piezoelectric moduli, which is symmetric in the last two indices (see, e.g., Ref. 9), ϵ_{il} is the tensor of dielectric susceptibility, and $\nu(\mathbf{q},a)$ is the unit polarization vector of the phonon branch a with the wave vector $\mathbf{q}$. The index q indicates the projection of a tensor on the $\mathbf{q}$ direction, while ρ is the mass density. For the deformation-potential interaction we have $W_\mathbf{q} = \pi\Lambda^2 q^2/\rho\omega_\mathbf{q}$, where Λ is the deformational-potential constant for the phonon branch under consideration. Using the approximate values for GaAs ($\beta = 0.16$ C m^{-2}, $\epsilon = 12$, $\Lambda = 8$ eV, $s = \omega_\mathbf{q}/q = 3\times10^5$ cm/s), we find that the piezoelectric interaction is the dominating one for frequencies $\omega_\mathbf{q} \lesssim 5\times10^{11}$ s^{-1}.

Let us investigate the consequences of the energy and quasimomentum conservation,

$$\epsilon_n(p+\hbar q_x) - \epsilon_{n'}(p) - \hbar\omega_\mathbf{q} = 0.$$

For the solution of this equation $p_{nn'}$ one has

$$p_{nn'} = \frac{m}{\cos\theta}\left(s - \frac{\Delta_{nn'}}{\hbar q}\right) - \frac{\hbar q\cos\theta}{2}, \quad (2)$$

where $s = \omega_\mathbf{q}/q$, θ is the angle between $\mathbf{q}$ and the x axis, and $\Delta_{nn'} = \epsilon_n^0 - \epsilon_{n'}^0$. Consequently, the delta function in Eq. (1) representing the energy and quasimomentum conservation can be expressed as $(m/\hbar q|\cos\theta|)\delta(p-p_{nn'})$.

Following the Landauer-Büttiker-Imry approach,[5] we express the equilibrium distribution functions of the reservoirs as $f_n^{(0)}(p) = f^{(\rm F)}[\epsilon_n(p) - \mu^{(\pm)}]$, where $f^{(\rm F)}$ is the Fermi function, $\mu^{(\pm)} = \mu \pm eV/2$, μ is the quasi-Fermi level (depending on the gate voltage), while V is the bias voltage. Consider the transitions involving a phonon with a given x component of the wave vector $q_x > 0$. Such a phonon can be emitted by a transition from an electron state having positive initial momentum $p+\hbar q_x$ to a state with negative momentum p (see Fig. 1). As a result, one gets[6]

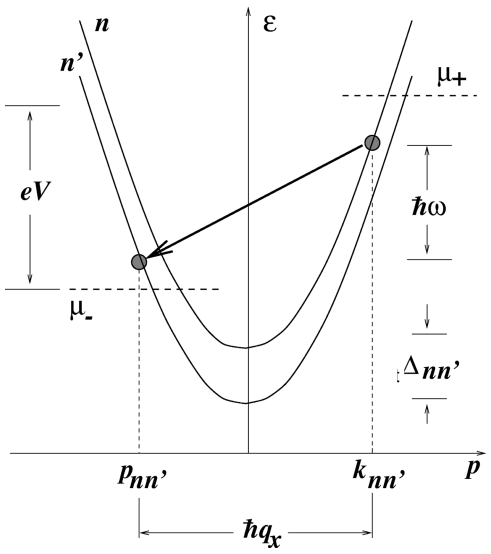

FIG. 1. Schematic representation of a transition from an electron state of subband n with energy ϵ and momentum $k_{nn'}$ to a state of subband n' with energy $\epsilon - \hbar\omega$ and momentum $p_{nn'} = k_{nn'} - \hbar q_x$.

$$\mathcal{R} = \frac{mW_\mathbf{q}}{\pi\mathcal{A}\hbar^2 q|\cos\theta|} \sum_{nn'} |C_{nn'}(\mathbf{q}_\perp)|^2 \times (f^{(\rm F)}[\epsilon_n(k_{nn'}) - \mu^{(+)}]\{1 - f^{(\rm F)}[\epsilon_{n'}(p_{nn'}) - \mu^{(-)}]\} \times (N_\mathbf{q}+1) - f^{(\rm F)}[\epsilon_{n'}(p_{nn'}) - \mu^{(-)}] \times \{1 - f^{(\rm F)}[\epsilon_n(k_{nn'}) - \mu^{(+)}]\}N_\mathbf{q}),$$

where $k_{nn'} = p_{nn'} + \hbar q_x$.

A. Intraband transitions

Let us start by considering transitions within the same subband. This is the dominating case for not too high phonon frequencies. For $n = n'$, the solution $p_{nn'}$ of Eq. (2) is n independent and equal to

$$p_1 = ms/\cos\theta - (1/2)\,\hbar q\cos\theta. \quad (3)$$

Thus, the $n = n'$ part of the collision operator can be rewritten as

$$\mathcal{R} = \frac{mW_\mathbf{q}}{\pi\mathcal{A}\hbar^2 q|\cos\theta|} \sum_n |C_{nn}(\mathbf{q}_\perp)|^2 \times [f_{nk_1}(1-f_{np_1})(N_\mathbf{q}+1) - f_{np_1}(1-f_{nk_1})N_\mathbf{q}], \quad (4)$$

where $k_1 = p_1 + hq_x = ms/\cos\theta + \hbar q_x/2$.

Let us consider the case $T = 0$ (or, to be more specific, $\hbar\omega_\mathbf{q} \gg k_{\rm B}T$). Then Eq. (4) yields

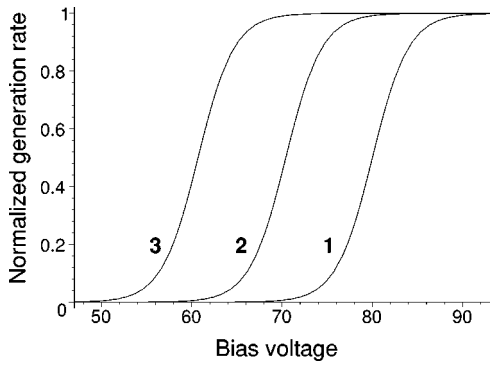

FIG. 2. Voltage dependencies of the normalized phonon-generation rate for intraband transitions $n \to n$ and different propagation angles. 1, $\theta = 0°$; 2, 30°; 3, 50°. The bias voltage is measured in units of $k_B T/e$. $\hbar\omega_{\mathbf{q}}/ms^2 = 6$, $ms^2/k_B T = 5$, $\mu/\epsilon_n^0 = 1$.

$$\mathcal{R} = \frac{mW_{\mathbf{q}}}{\pi \mathcal{A} \hbar^2 q |\cos\theta|} \sum_n |C_{nn}(\mathbf{q}_\perp)|^2 \times \theta[\mu^{(+)} - \epsilon_n(k_1)]\,\theta[\epsilon_n(p_1) - \mu^{(-)}].$$

One can easily see that a *current-carrying channel can generate phonons*. Since p_1 must be negative, Eq. (3) leads to the inequality

$$\cos^2\theta > 2ms^2/\hbar\omega_{\mathbf{q}}, \tag{5}$$

which defines an upper limit for the propagation angle. Since $\epsilon_n(k_1) - \epsilon_n(p_1) = \hbar\omega_{\mathbf{q}}$, $\mu^{(+)} - \mu^{(-)} = eV$, and $|\cos\theta| \leqslant 1$, the phonon generation is restricted to frequencies $\omega_{\mathbf{q}}$ satisfying the inequalities

$$2ms^2 < \hbar\omega_{\mathbf{q}} < eV. \tag{6}$$

The condition $\hbar\omega_{\mathbf{q}} < eV$ has been indicated earlier for the case of electrophonon resonance in nanostructures.[11]

The frequency region given by Eq. (6) is further restricted by the Pauli principle via occupation numbers for the initial and final states. The latter depend on the position of the quasi-Fermi level μ, which in its turn is controlled by the gate voltage. Let us consider intraband transitions within a given subband n. The limitation is expressed by the inequalities $\epsilon_1 + \hbar\omega_{\mathbf{q}} - eV/2 < \mu < \epsilon_1 + eV/2$, where $\epsilon_1 \equiv \epsilon_n[p_1(\omega_{\mathbf{q}}, \theta)]$. Consequently, if Eq. (5) is satisfied, then phonons with frequency $\omega_{\mathbf{q}}$ and propagation direction θ are generated provided the bias voltage exceeds the threshold given by

$$eV > 2\max(\mu - \epsilon_1, \epsilon_1 + \hbar\omega_{\mathbf{q}} - \mu). \tag{7}$$

Let us investigate the frequency region in which phonon generation is possible at least at some angle for a given μ and V. If $\hbar\omega_{\mathbf{q}} > 2ms^2$, then the function $[p_1(\omega_{\mathbf{q}}, \theta)]^2/2m$ varies between the value $(\hbar\omega_{\mathbf{q}} - 2ms^2)^2/8ms^2$ and zero as the angle θ goes from zero to the upper limit from Eq. (5). We may thus summarize the above inequalities by stating that phonon generation from transitions within the subband n will take place (for at least some propagation angles) in the frequency range

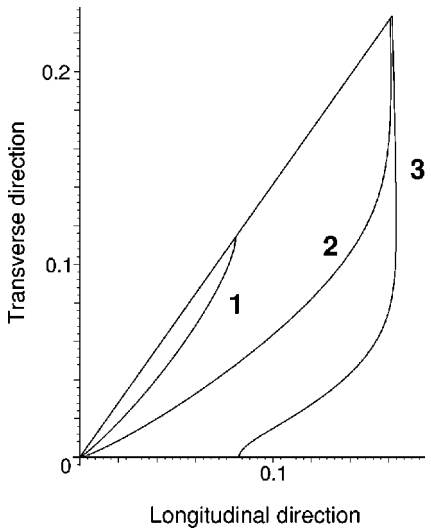

FIG. 3. Angular dependencies of the phonon generation rate for intraband transitions $n \to n$ and voltages near the threshold. 1, $eV/k_B T = 60$; 2, 70; 3, 80. The upper-limiting angle corresponds to the condition $p_1 < 0$ [see Eq. (5)]. The rate is measured in units of $W_{\mathbf{q}}/\pi\mathcal{A}\hbar s$. Other values of the parameters are the same as in Fig. 2. We neglect the angular dependence of the coupling parameter $W_{\mathbf{q}}$.

$$2ms^2 + \sqrt{8ms^2(\mu - eV/2 - \epsilon_n^0)}\,\Theta(\mu - eV/2 - \epsilon_n^0) < \hbar\omega_{\mathbf{q}} < \min(eV, \mu + eV/2 - \epsilon_n^0).$$

In Fig. 2 the dependence of the phonon emission rate $\mathcal{R}$ on the bias voltage is shown. Thresholds in the bias voltage are apparent. If the voltage is further increased, new subbands will contribute to the phonon emission [see Eq. (7)]. Consequently, the generation rate is a steplike function of the bias voltage. There will be equally high steps corresponding to intraband transitions, and a small modification from interband transitions. The typical rate (corresponding to each step) is $\mathcal{R} = (ms/\hbar q|\cos\theta|)\mathcal{R}_0$ with $\mathcal{R}_0 = W_{\mathbf{q}}/\pi\mathcal{A}\hbar s$. Assuming $\beta^2/\epsilon\epsilon_0\rho s^2 = 5 \times 10^{-3}$, $\hbar q/ms = 6$, $s = 3 \times 10^5$ cm/s, $m = 0.07 m_0$, $\mathcal{A} = 10^{-12}$ cm^2, $\epsilon = 12$, we get $\mathcal{R}_0 \approx 10^{13}$ s^{-1}. We assume that $qd \lesssim 1$, where d is the width of the channel. Thus, $|C_{nn}(\mathbf{q}_\perp)|^2 \approx 1$, independently of the shape of the channel.

Angular dependencies of the generation rate near the voltage threshold are shown in Fig. 3. It is seen that the character of the angular dependence is changed at the threshold. There is a sharp cutoff at the upper-limiting angle corresponding to $p_1(\omega_{\mathbf{q}}, \theta) = 0$ [see Eq. (5)]. This cutoff could be made more realistic (that is, smoother) by taking into account the scattering of electrons by a short-range impurity potential. As was shown in Ref. 12, such a potential has the effect of a smearing of the momentum-conservation law. Furthermore, we have neglected the angular dependence of the coupling constant $W_{\mathbf{q}}$, which depends on the acoustic properties of the substrate. This additional dependence should be multiplied to obtain the observed angular dependence.

B. Interband transitions

The phonons can also be emitted by interband transitions. Below we consider transitions from states belonging to a

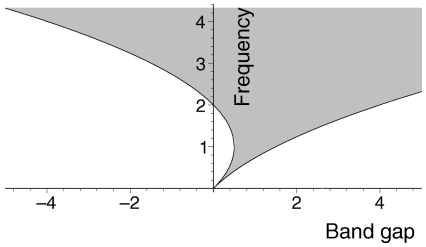

FIG. 4. The shaded region corresponds to the frequency region defined by Eqs. (9). There is no phonon generation for frequencies in the unshaded region. The phonon frequency ($\omega_{\mathbf{q}}$) is measured in units of $ms^2/\hbar$, the band gap ($\Delta_{nn'}$) in units of ms^2.

subband n to states of a different subband n'. The frequency regions in which such processes may occur are different from those for intraband transitions, although the inequality $\hbar\omega_{\mathbf{q}}<eV$ remains. The possible propagation angles are further restricted by the angular dependence of the factor $|C_{nn'}(\mathbf{q}_\perp)|^2$. Since we assume that $q_\perp d\lesssim 1$ (d being the channel width), interband transitions are suppressed by this factor for all directions. However, as will be shown, they bear an additional information comparing to the intraband transitions.

The final electron momentum $p_{nn'}$ must be negative, as before, but is now given by Eq. (2). Furthermore, the initial momentum $k_{nn'}=p_{nn'}+\hbar q\cos\theta$ must be positive. This yields the condition

$$\cos^2\theta>(2ms^2/\hbar\omega_{\mathbf{q}})|1-\Delta_{nn'}/\hbar\omega_{\mathbf{q}}|, \tag{8}$$

which replaces Eq. (5) for the upper-limiting propagation angle. In addition there is a voltage threshold given by Eq. (7), where ϵ_1 now stands for $\epsilon_{n'}[p_{nn'}(\omega_{\mathbf{q}},\theta)]$.

Phonon generation is only possible at frequencies for which the right-hand side of Eq. (8) is less than 1, which occurs when

$$\begin{aligned}
&\hbar\omega_{\mathbf{q}}>\epsilon_{++-} && \text{if} \quad \Delta_{nn'}<0,\\
&\hbar\omega_{\mathbf{q}}>\epsilon_{++-} \quad \text{or} \quad \epsilon_{+--}>\hbar\omega_{\mathbf{q}}>\epsilon_{-++} && \text{if} \quad 0<\Delta_{nn'}<ms^2/2,\\
&\hbar\omega_{\mathbf{q}}>\epsilon_{-++} && \text{if} \quad ms^2/2<\Delta_{nn'},
\end{aligned} \tag{9}$$

with $\epsilon_{\pm\pm\pm}=\pm ms^2\pm\sqrt{ms^2(ms^2\pm 2\Delta_{nn'})}$. This frequency region corresponds to the shaded area in the $\omega_{\mathbf{q}}$–$\Delta_{nn'}$ diagram of Fig. 4. Since usually $|\Delta_{nn'}|\gg ms^2$, phonon generation is restricted by the inequalities

$$\sqrt{2ms^2|\Delta_{nn'}|}\lesssim\hbar\omega_{\mathbf{q}}<eV.$$

In Fig. 5 one can see the angular dependencies of the generation rate for three different values of the applied voltage. They are not quite similar to the case of intraband transitions. There is no phonon emission in the forward direction, because the matrix element $C_{nn'}(\mathbf{q}_\perp)$ vanishes for $\theta=0$. The threshold values of voltage are shifted. Furthermore, the upper-limiting angle is in this case due to the condition that the initial momentum $k_{nn'}(\omega_{\mathbf{q}},\theta)$ must be positive. The final momentum $p(\omega_{\mathbf{q}},\theta)$, on the other hand, is negative for all angles, given these parameters.

III. NONUNIFORM CHANNEL

The edges of the channel play a specific role. Namely, if the shape of the channel is smooth enough, as we assume here, one can use the so-called adiabatic approach,[13] i.e., describe the situation in terms of a position-dependent band structure. We will show that the phonons with a given frequency and propagation direction can be generated only near specific points where the local energy and quasimomentum conservation laws are met. Consequently, the phonons emitted from the edges bear information about the position-dependent band gaps between the modes of transverse quantization.

Consider an adiabatic quantum channel with the width depending on coordinate x. The electron wave functions for such channels can be subdivided into two categories—the propagating states and the reflected states on each side. For the propagating state directed to the right ($p>0$), one has

$$\psi_{\rightarrow}(\mathbf{r})=\left|\frac{p}{p(x)\mathcal{L}}\right|^{1/2}\chi_{nx}(\mathbf{r}_\perp)\exp\left[\frac{i}{\hbar}\int^x p(x')dx'\right].$$

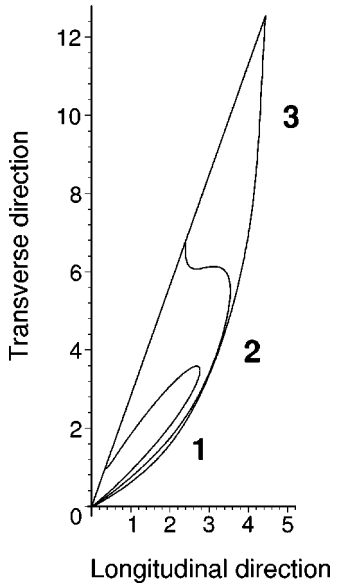

FIG. 5. Angular dependencies of the phonon generation rate in the interface plane for interband transitions $n\rightarrow n'=n-1$ and different voltages. 1, $eV/k_BT=35$; 2, 40; 3, 45. The upper-limiting angle corresponds to the condition $k_{nn'}>0$ [see Eq. (8)]. The rate is measured in units of $(qd)^2W_{\mathbf{q}}/10^3\pi\mathcal{A}\hbar s$. Furthermore, $\Delta_{nn'}/ms^2=+8$, and $\mu=\epsilon_n^0-\Delta_{nn'}/4$. Other values of the parameters are the same as in Fig. 3.

In this expression, the transverse wave functions χ_n as well as the corresponding eigenvalues ϵ_n^0 are assumed to vary slowly with the longitudinal coordinate x. The longitudinal quasimomentum $p(x)\equiv p_n(x;\epsilon)$ is defined by $p(x)^2/2m + \epsilon_n^0(x) = \epsilon > \max\{\epsilon_n^0(x)\}$, while $p\equiv\sqrt{2m\epsilon}$ is the value at infinity $x\to\pm\infty$. Thus, $\epsilon_n^0(x)\equiv\epsilon_n(p=0;x)$ is the local position of the bottom of the nth 1D transverse band at the point x. We assume that the functions ϵ_n^0 decrease monotonically and symmetrically to zero in both directions from the maximum point at $x=0$. The oppositely directed propagating state $\psi_{\leftarrow}$ is defined in the same way, but with negative quasimomentum $p(x)$.

For a totally reflected electron state on the left-hand side of the channel, $\epsilon<\max\{\epsilon_n^0(x)\}=\epsilon_n^0(0)$, the wave function is

$$\psi_{\hookleftarrow}(\mathbf{r})=\left|\frac{2p}{p(x)\mathcal{L}}\right|^{1/2}\chi_{nx}(\mathbf{r}_\perp)\sin\left[\frac{1}{\hbar}\int_{x_t}^{x}p(x')dx'\right],$$

x_t being the classical turning point.[14] A reflected state on the right-hand side of the channel is denoted by $\psi_{\hookrightarrow}$. Below we will characterize the electronic state by the combination $\alpha=\{n,p\}$ together with a subscript $s=\rightarrow,\leftarrow,\hookleftarrow$, or $\hookrightarrow$.

As we are dealing with a nonuniform channel, we must take into account the effect of screening. The electrons in the wide regions of the channel are more mobile than those in the narrow regions. Therefore, the screening of the electron-phonon interaction, and thus the coupling strength, will depend on the position. We may take this effect into account by multiplying the function $\exp(-i\mathbf{q}\cdot\mathbf{r})$ in the transition amplitudes by a dimensionless factor $\eta(\mathbf{r})$. This factor, which will be less than 1, is determined by the screening of the piezoelectric field or deformation potential field by the electrons inside the leads and the channel. In the 2D leads, $\eta(\mathbf{r})$ is small because of the high conductance of the 2DEG. However, if the channel width is of the order of the effective Bohr radius $\epsilon\epsilon_0\hbar^2/me^2$, then the screening inside the channel is not too strong. The screening of the effective field in realistic gated structures is far from being satisfactory understood, the more so that we are actually dealing with a nonstationary effect. However, there are indications that the effective potential is not much lower than the unscreened one (see, e.g., Ref. 15), and we shall assume this throughout the paper. In a narrow channel and at $q\mathcal{L}\gg1$ (here we denote by $\mathcal{L}$ the effective length of the channel), one can consider $\eta(\mathbf{r})$ as a smooth function $\eta(x)$ inside the channel and rapidly decreasing outside.

Another simplification that arises from the above inequality is that one can employ the *stationary-phase approximation* for estimation of the transition probabilities. For two propagating states $\alpha_s=\{n,p_\alpha\}_s$ and $\beta_{s'}=\{n',p_\beta\}_{s'}$, the transition amplitude is

$$\langle\beta_{s'}|\,\eta(x)\exp(-i\mathbf{q}\cdot\mathbf{r})|\alpha_s\rangle=\int_{-\infty}^{\infty}dx\,A(x)\exp[i\varphi(x)],\tag{10}$$

where $A(x)$ is a result of the integration in the transverse directions, while the x-dependent part of the integrand's phase is given by

$$\varphi(x)\equiv\varphi_{\alpha s,\beta s'}(x)=\hbar^{-1}\int^{x}[p_\alpha(x')-p_\beta(x')]dx'-q_x x.$$

Here $p_\alpha(x)$ is determined as the solution p of the equation $\epsilon_n(p,x)=p_\alpha^2/2m(=\epsilon_\alpha)$. With one or both of the states being reflected ones, we get two or four terms in the transition amplitude, respectively. Now the phase $\varphi(x)$ is expanded around a stationary point x^* defined by the equation $d\varphi/dx=0$,

$$\varphi(x)=\varphi(x^*)+\varphi''(x^*)(x-x^*)^2/2.\tag{11}$$

If such a stationary point x^* exists for φ, then the main contribution to the integral is concentrated around this point. As the part $A(x)$ of the integrand is assumed to vary slowly on the scale $\sim\sqrt{2/|\varphi''(x^*)|}$, one can substitute $A(x)$ in the integrand by $A(x^*)$. If φ has no stationary points, one assumes a rapidly oscillating phase everywhere, thus the total contribution to the transition amplitude is much smaller than above.

In this picture, the transitions are localized at the points x^* where $\varphi'(x^*)=0$. In our case, the change in energy $\epsilon_\alpha = \epsilon\to\epsilon_\beta=\epsilon-\hbar\omega_{\mathbf{q}}$ due to emission of a phonon is accompanied by a quasimomentum transfer $-\hbar q_x$, i.e., at the point of stationary phase one arrives at the *local conservation condition*

$$p_n(x^*;\epsilon)=p_{n'}(x^*;\epsilon-\hbar\omega_{\mathbf{q}})+\hbar q_x.\tag{12}$$

We would like to emphasize once again that the *local* values of quasimomentum entering Eq. (12)—rather than the asymptotic values p—determine the conservation law.

The above approach has been employed to analyze the photoconductance[16] and the acoustoconductance[17] in an adiabatic quantum channel.

A. Phonon generation

The transition amplitude of Eq. (10) is given by

$$\langle\beta_{s'}|\,\eta(x)e^{-i\mathbf{q}\cdot\mathbf{r}}|\alpha_s\rangle = \int_{-\infty}^{\infty}dx C_{nn'}(\mathbf{q}_\perp,x)\,\tilde{\eta}_{\alpha s,\beta s'}(x)\exp[i\varphi_{\alpha s,\beta s'}(x)],$$

where $C_{nn'}$ depends (smoothly) on x through the transverse functions χ_{nx}, while

$$\tilde{\eta}_{\alpha s,\beta s'}(x)\equiv\eta(x)\xi_s\xi_{s'}|p_\alpha p_\beta/p_\alpha(x)p_\beta(x)\mathcal{L}^2|^{1/2}.$$

The factor ξ_s is 1 for propagating states, $\pm i/\sqrt{2}$ for reflected ones. In the stationary phase approximation, the functions $C_{nn'}(\mathbf{q}_\perp,x)$ and $\tilde{\eta}_{\alpha s,\beta s'}(x)$ are replaced by their values at the stationary point $x^*_{\alpha s,\beta s'}$. Writing

$$\Phi_{\alpha s,\beta s'}\equiv\int_{-\infty}^{\infty}\exp[i\varphi_{\alpha s,\beta s'}(x)]dx,$$

we get for the generation rate of the nonuniform channel

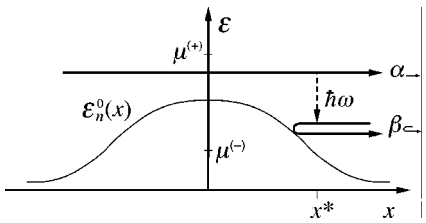

FIG. 6. Phonon emission in a nonuniform channel by a transition from a propagating to a reflected electron state. The transition is localized around the point x^*.

$$\mathcal{R}=(2W_{\mathbf{q}}/\mathcal{V})\sum_{\alpha s,\beta s'}|\Phi_{\alpha s,\beta s'}|^2|\tilde{\eta}_{\alpha s,\beta s'}(x^*_{\alpha s,\beta s'})|^2 \times|C_{nn'}(\mathbf{q}_\perp,x^*_{\alpha s,\beta s'})|^2[f_{\alpha s}(1-f_{\beta s'})(N_{\mathbf{q}}+1) - f_{\beta s'}(1-f_{\alpha s})N_{\mathbf{q}}]\delta(\epsilon_\alpha-\epsilon_\beta-\hbar\omega_{\mathbf{q}}), \tag{13}$$

where $\mathcal{V}$ is the interaction volume (which is not known precisely, but is of the order of the geometrical volume of the channel). The point x^* and the phase $\varphi(x)$ are dependent on α_s and $\beta_{s'}$. However, to avoid excessive proliferation of indices we will often omit these indices.

Now assuming that the second-order term in the expansion (11) of the phase grows faster to values of the order 1 than the following terms [i.e., at $|\varphi'''(x^*)/\varphi''(x^*)^{3/2}|\ll 1$], the factor $\Phi_{\alpha s,\beta s'}$ can be evaluated as

$$\Phi_{\alpha s,\beta s'}=|2\pi/\varphi''(x^*)|^{1/2} \times\exp[i\varphi(x^*)+i(\pi/4)\ \ \mathrm{sgn}\,\varphi''(x^*)],$$

where $\mathrm{sgn}\,x=x/|x|$. The quasimomenta $p_\alpha(x^*)$ and $p_\beta(x^*)$ at the transition point are fixed by the conditions

$$\epsilon^0_n(x^*)+p_\alpha(x^*)^2/2m=\epsilon^0_{n'}(x^*)+p_\beta(x^*)^2/2m+\hbar\omega_{\mathbf{q}},$$

$$p_\alpha(x^*)=p_\beta(x^*)+\hbar q_x.$$

They can be positive or negative. In the case of one or both of the involved states being reflected ones, the transition amplitude falls into two or four parts, respectively, since a reflected state is a superposition of waves with $p>0$ and $p<0$. However, if $n=n'$, a stationary point x^* exists for at most one of these terms, and we denote by $+p_{\alpha(\beta)}$ the momentum with the corresponding sign.

B. Intraband transitions

For $n=n'$ we have

$$p_\alpha(x^*)=k_1\equiv ms/\cos\theta+\hbar q_x/2,$$

$$p_\beta(x^*)=p_1\equiv ms/\cos\theta-\hbar q_x/2. \tag{14}$$

The quasimomenta at the transition point are the same as in the case of a uniform channel. However, the electron energy ϵ_α is no longer fixed by the phonon $(\omega,\mathbf{q})$, since there are now different solutions x^* of Eqs. (14) corresponding to different energies $\epsilon_\alpha=\epsilon^0_n(x^*)+k_1^2/2m$.

Let us again assume $T=0$. Then the only possible phonon-generating processes are the ones shown in Figs. 6 and 7. Thus, in Eq. (13) we have $s=\rightarrow$, while $s'=\leftarrow$ [if $\epsilon_\alpha-\hbar\omega_{\mathbf{q}}>\epsilon^0_n(0)$] or $s'=\hookrightarrow$ [if $\epsilon_\alpha-\hbar\omega_{\mathbf{q}}<\epsilon^0_n(0)$]. Introducing the density of states $g(\epsilon)$, we get

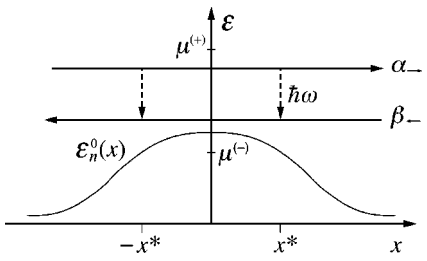

FIG. 7. Phonon emission in a nonuniform channel by a transition between two oppositely directed propagating states. There are two transition points.

$$\mathcal{R}=(2W_{\mathbf{q}}/\mathcal{V})\sum_n\int d\epsilon g(\epsilon)g(\epsilon-\hbar\omega_{\mathbf{q}}) \times|\Phi_{n\epsilon}|^2|\tilde{\eta}_{n\epsilon}(x^*_{n\epsilon})|^2|C_{nn}(\mathbf{q}_\perp,x^*_{n\epsilon})|^2 \times\Theta(\mu^{(+)}-\epsilon)\Theta(\epsilon-\hbar\omega_{\mathbf{q}}-\mu^{(-)}), \tag{15}$$

where the following three restrictions are implied: (i) A transition point x^* must really exist for the energy ϵ involved, which is only the case when $k_1^2/2m<\epsilon<k_1^2/2m+\epsilon^0_n(0)$. (ii) The initial state must be propagating, thus $\epsilon^0_n(0)<\epsilon$. (iii) For a transition between propagating states (Fig. 7), the final one must be propagating to the left. This means that $p_1<0$, which, as before, leads to Eq. (5), and hence the condition $\hbar\omega_{\mathbf{q}}>2ms^2$, for such transitions. However, for transitions to a nonpropagating state (Fig. 6), there is no such restriction.

For a transition of the kind in Fig. 7, there will in fact be *two* transition points, one on each side of the constriction (cf. with Ref. 18). The corresponding two parts of the transition amplitude give rise to the interference term $2\{1+\sin[\varphi(x^*)-\varphi(-x^*)]\}$.

If, as in the case of a parabolic or square-confining potential, the transverse energy has the form $\epsilon^0_n(x)=\alpha_n/d(x)^2$, $d(x)$ being the width of the channel, then

$$\varphi''(x^*)=\frac{p'_\alpha(x^*)-p'_\beta(x^*)}{\hbar}=\frac{2mq_x\epsilon^0_n(x^*)}{p_1k_1}\frac{d'(x^*)}{d(x^*)}.$$

Inserting these expressions and $g(\epsilon)=\mathcal{L}\sqrt{m}/h\sqrt{2\epsilon}$ into Eq. (15), we finally get

$$\mathcal{R}=\frac{mW_{\mathbf{q}}}{\pi\mathcal{V}\hbar^2q|\cos\theta|} \times\sum_n\int d\epsilon\frac{\eta^2(x^*_{n\epsilon})|C_{nn}(q_\perp,x^*_{n\epsilon})|^2d(x^*_{n\epsilon})}{\epsilon^0_n(x^*_{n\epsilon})|d'(x^*_{n\epsilon})|}\nu_n(\epsilon), \tag{16}$$

where the integration goes from $\max(k_1^2/2m,\epsilon^0_n(0),\mu^{(-)}+\hbar\omega_{\mathbf{q}})$ to $\min(k_1^2/2m+\epsilon^0_n(0),\mu^{(+)})$, and $\nu_n(\epsilon)$ represents the interference part. This function is given by

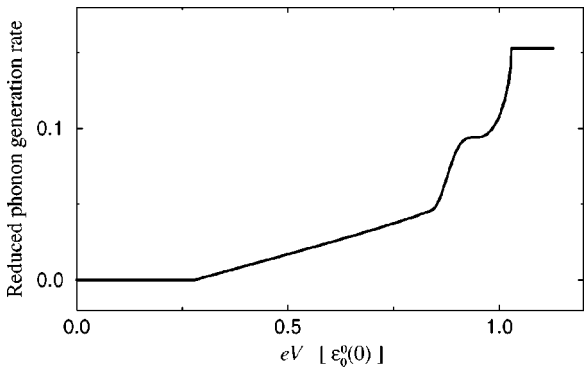

FIG. 8. Dependence of the phonon generation rate $\mathcal{R}$ in a nonuniform channel on the bias voltage V, corresponding to intraband transitions of the zeroth subband ($n=0$). Phonon generation sets on when eV exceeds $\hbar\omega_{\mathbf{q}}$ and increases approximately linearly, corresponding to transitions like the one in Fig. 6. In regions where transitions between propagating states are possible as well (Fig. 7), the generation rate increases nonlinearly, corresponding to the interference connected with these processes. When $\mu^{(+)}=\mu+eV/2$ becomes large enough, no further transitions are possible, and the generation rate stays constant until the onset of contributions from the next subband (not shown). Here, the channel width is assumed to vary as $d(x)=d(1+x^2/a^2)$ with a parabolic transverse confining potential. Thus, $\epsilon_n^0(x)=\epsilon_0^0(0)(2n+1)(1+x^2/a^2)^{-2}$, with the zeroth transverse energy maximum $\epsilon_0^0(0)=\hbar^2/2md^2$. The generation rate is shown in units of $mW_{\mathbf{q}}\eta^2 a/\mathcal{V}\hbar^2 q$, the bias voltage in units of $\epsilon_0^0(0)/e$. The screening factor η is set constant for simplicity. The quasi-Fermi level μ is chosen such that $\mu^{(+)}=\epsilon_0^0(0)$ when $eV=\hbar\omega_{\mathbf{q}}$. Furthermore, $d=0.08$ μm, $a=6$ μm, $m=0.07m_0$, $s=3\times10^5$ cm/s, $q=6ms/\hbar$, and $\theta=0$.

$$\nu_n(\epsilon)=\left\{1+\sin\left[2\hbar^{-1}\int_0^{x^*}dx[|p_n(x;\epsilon)| + |p_n(x;\epsilon-\hbar\omega_{\mathbf{q}})|-\hbar q_x]\right]\right\}\Theta(\hbar\omega_{\mathbf{q}}\cos^2\theta-2ms^2)$$

if $\epsilon>\epsilon_n^0(0)+\hbar\omega_{\mathbf{q}}$, otherwise $\nu_n(\epsilon)=1/4$. As before, the Fermi functions $f^{(\mathrm{F})}(\varepsilon)\to\Theta(-\varepsilon)$ in Eq. (15) cause the condition $\hbar\omega_{\mathbf{q}}<eV$.

When the energy ϵ approaches $k_1^2/2m$ (from above) or $\epsilon_n^0(0)+k_1^2/2m$ (from below), the transition point $x_{n\epsilon}^*$ approaches infinity or zero, respectively. At these energies, which correspond to regions where the stationary-phase approximation is not valid, $\epsilon_n^0(x^*)$ and $d'(x^*)$, respectively, approach zero, making the integrand in Eq. (16) diverge. However, these energy regions make up only two narrow parts of the integration range, and the integral itself converges.

Figure 8 shows the dependence of the generation rate on the bias voltage for a set of typical parameters. The phonon generation sets on for $eV=\hbar\omega_{\mathbf{q}}$ and, in contrast to the case of a uniform channel, increases approximately linearly: As eV increases, more and more phonon-emitting transitions become possible, since the energies of the involved electrons is not fixed. Figure 9 shows the variation of the differential generation rate with the bias voltage. It is proportional to the integrand of Eq. (16) with ϵ replaced by $\mu^{(+)}$. The slowly varying part corresponds to transitions from propagating to reflected states, while the oscillating part corresponds to transitions between oppositely directed propagating states.

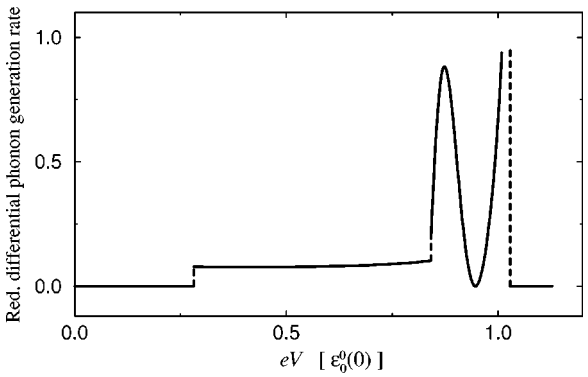

FIG. 9. Dependence of the differential generation rate $\mathcal{R}$ [shown in units of $mW_{\mathbf{q}}e\eta^2 a/\mathcal{V}\hbar q\epsilon_0^0(0)$] on the gate voltage V [in units of $\epsilon_0^0(0)/e$]. The differential rate is not continuous at the points where the transitions change character. Furthermore, it diverges (in this approximation) for $\mu^{(+)}\to k_1^2/2m+\epsilon_0^0(0)$. The parameters are the same as for Fig. 8.

It is important to note that the two patterns of phonon generation considered in this paper are physically different. The first one (Sec. II) involves transitions that take place homogeneously inside the whole channel (quantum wire). The pattern considered in this section, on the other hand, involves transitions only near the edges of the channel, where the conservation laws are local and thus different from the ones for the uniform part. As a result, phonons with $\hbar q<2ms$ can be generated. Observations of such phonons can be an indication of the importance of the processes near the edges. An effective interaction length in this case is $l(x^*)=|d(x^*)/d'(x^*)|$. An estimate of the relative intensity of those processes compared to uniform generation is given by $\min[l(x^*)/\mathcal{L},1]$, where $\mathcal{L}$ is the approximate channel length.

In this section, we have considered the case of intraband transitions in a nonuniform channel. The calculations in the interband case ($n\neq n'$) are similar, but more complicated, and will not be carried out here. However, the main effects discussed above, i.e., interference and the possibility to discriminate between different kinds of transitions, are relevant to that case as well. Also, as in the case of interband transitions in a uniform channel (Sec. II B), there are voltage thresholds in the phonon-generation rate. Due to the x dependence of the band gap $\Delta_{nn'}(x)$, these thresholds are less pronounced.

Phonon generation is accompanied by non-Ohmic behavior of the conductance. This was analyzed for optical phonons in Ref. 11. For the case of acoustical phonons it needs both additional experimental and theoretical investigation.

We have discussed the generation of bulk phonons. However, the same methods can be applied for the investigation of the generation of elastic modes confined to the interfaces.

IV. CONCLUSION

We have calculated the rate of phonon generation by a current-carrying quantum channel. The generation rate is a steplike function of the applied bias voltage. The threshold

voltages are directly related to the band gaps between the modes of transverse quantization, while the generation rates at the plateaus are related to the electron-phonon coupling constant inside the channel. The emitted phonons have a characteristic angular distribution with a cutoff at an upper-limiting angle. The rate corresponding to phonons that are generated near the edges has a characteristic voltage dependence that is sensitive to the shape of the channel.

In conclusion, we shown that the spectral and spatial distributions of emitted phonons as well as the dependence of the generation rate on the bias voltage bear information both on electron-phonon coupling in the quantum channel and on characteristics of the electron spectrum.

ACKNOWLEDGMENTS

V.L.G. is grateful to the University of Oslo for hospitality and financial support of this work. His work was also partially supported by the Russian National Fund of Fundamental Research (Grant No. 97-02-18236-a). H.T. is grateful to the Norwegian Research Council for financial support.

[1] A. J. Kent, A. J. Naylor, P. Hawker, M. Henini, and B. Bracher, Phys. Rev. B **55**, 9775 (1997).

[2] V. I. Talyanskii, J. M. Shilton, J. Cunningham, M. Pepper, C. J. B. Ford, C. G. Smith, E. H. Linfield, D. A. Ritchie, and G. A. C. Jones, Physica B **251**, 140 (1998).

[3] S. Roshko, W. Dietsche, and L. J. Challis, Phys. Rev. Lett. **80**, 3835 (1998).

[4] E. Chow, H. P. Wei, S. M. Girvin, and M. Shayegan, Phys. Rev. Lett. **77**, 1143 (1996).

[5] R. Landauer, IBM J Res. Dev. **1**, 233 (1957); **32**, 306 (1989); Y. Imry, in *Directions in Condensed Matter Physics*, edited by G. Grinstein and G. Mazenko (World Scientific, Singapore, 1986), p. 101; M. Büttiker, Phys. Rev. Lett. **57**, 1761 (1986).

[6] V. L. Gurevich, Phys. Rev. B **55**, 4522 (1997).

[7] I. O. Kulik, R. I. Shekhter, and A. N. Omelyanchouk, Solid State Commun. **23**, 301 (1977), pointed out that the processes leading to electric resistance and heat generation are spatially separated in a classical point contact.

[8] N. Nishiguchi, Y. Ando, and M. N. Wybourne, J. Phys. Condens. Matter **9**, 5751 (1997).

[9] V. L. Gurevich, *Transport in Phonon Systems* (North-Holland, Amsterdam, 1986).

[10] V. L. Gurevich, V. B. Pevzner, and G. J. Iafrate, Phys. Rev. Lett. **77**, 3881 (1996).

[11] V. L. Gurevich, V. B. Pevzner, and G. J. Iafrate, Phys. Rev. Lett. **75**, 1352 (1995); J. Phys. Condens. Matter **7**, L445 (1995).

[12] Ø. L. Bø , H. Totland, and Yu. Galperin, J. Phys.: Condens. Matter **9**, 8381 (1997).

[13] L. I. Glazman, G. B. Lesovik, D. E. Khmel'nitskii, and R. I. Shekhter, Pis'ma Zh. Eksp. Teor. Fiz. **48**, 218 (1988) [JETP Lett. **48**, 238 (1988)].

[14] We assume the amount of *partially* reflected states is small.

[15] A. Wixforth, J. Scriba, M. Wassermeier, J. P. Kotthaus, G. Weimann, and W. Schlapp, Phys. Rev. B **40**, 7874 (1989).

[16] A. Grincwajg, L. Y. Gorelik, V. Z. Kleiner, and R. I. Shekhter, Phys. Rev. B **52**, 12 168 (1995).

[17] H. Totland, Ø. L. Bø, and Yu. M. Galperin, Phys. Rev. B **56**, 15 299 (1997).

[18] F. A. Maaø and Y. M. Galperin, Phys. Rev. B **56**, 4028 (1997).